

Design of Nonlinear Resonator Arrays in Superconducting Circuits

Lukas Korosec

August 29, 2012

Contents

1	Introduction	4
2	Theory	5
2.1	Photon Blockade	5
2.2	Parametric Drives	5
3	Components	7
3.1	Resonator	7
3.2	Qubits	7
3.3	Flux Gatelines	7
3.4	Charge Gatelines	8
3.5	Airbridges	8
4	Mask Design with Mathematica	9
4.1	Semiautomatic Gateline Placement	9
4.2	“Black Boxes”	9
4.3	Mask Completion for Ordering	11
5	The Samples	12
6	Conclusion and Prospect	25

Circuit Quantum Electrodynamics (QED) provides an architecture to perform Cavity QED experiments with a superconducting microwave circuit. Several experiments on this subject already have been successfully conducted by the Quantum Device Lab at ETH Zurich, using samples written using photolithography and electron beam lithography. The masks for photolithography are designed using Mathematica. In this work I will describe the design of several of these masks, that will be used to produce samples with which it is expected to be able to observe Majorana bound states of light [1].

1 Introduction

Circuit Quantum Electrodynamics (cQED) provides an architecture for studying the interaction between light and matter on a chip. The macroscopic circuits behave quantum mechanically as single atoms coupling to the electric field in a cavity. It is a promising candidate for quantum computing [2, 3].

The Quantum Device Lab at ETH Zurich has successfully implemented Circuit QED by creating samples consisting of superconducting aluminum and niobium structures on a sapphire substrate.

The samples are produced by taking a sapphire wafer coated with aluminum and removing small parts of the aluminum using photolithography. If a structure cannot be written using photolithography because e.g. it is too small, it can be produced by means of electron beam (e-beam) lithography, creating a niobium structure on the sapphire substrate, after removing the aluminum in the area around it using photolithography.

The masks for the photolithography are designed using 3D graphics produced in Mathematica, only the final few steps require more advanced CAD software. The Quantum Device Lab has developed a library for Mathematica specifically for mask design.

The goal of this semester project was to design a set of masks for photolithography for a series of samples for experiments based on the ideas presented by Bardyn et al. [1] for observing Majorana bound states of light. This can be realized by creating a chain of several nonlinear microwave resonators that are coupled to qubits which creates photon blockade system and connecting the resonators to one another using parametric drives that will emit a single photon into each adjacent resonator simultaneously.

2 Theory

This section will provide a basic explanation of the theoretical considerations behind the devices that will be found on the designed samples.

2.1 Photon Blockade

The coupling of a cavity and a two-level system (qubit) with a finite electric dipole moment will result in a non-linear splitting of the energy levels of the cavity. The system is described by the Jaynes-Cummings model, given by the Hamiltonian

$$H = \hbar\omega(a^\dagger a + \frac{1}{2}) + \hbar\omega_A \frac{\sigma_z}{2} + \hbar g(a\sigma_+ + a^\dagger\sigma_-) \quad ,$$

where ω is the resonance frequency of the cavity, ω_A is the resonance frequency of the qubit, g is the coupling strength between the cavity and the qubit, a and a^\dagger are the creation and annihilation operators of the cavity, and σ_z , σ_+ and σ_- are the respective Pauli matrix and ladder operators acting on the states of the qubit.

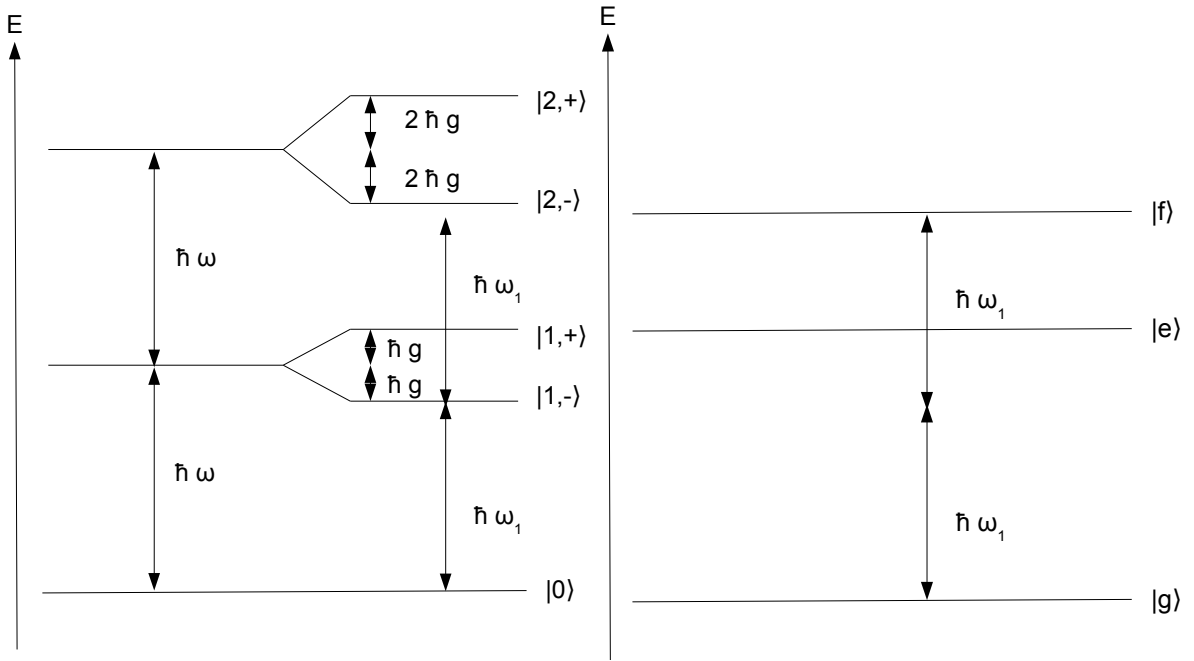
When the qubit is in resonance with the cavity, i.e. $\omega = \omega_A$, the resulting energy levels are

$$E_{n,\pm} = \hbar\omega(n + \frac{1}{2}) \pm \hbar g\sqrt{n}, \quad n=0,1,2,\dots$$

as sketched in Figure 2.1a. This energy level scheme is strongly non-linear for large coupling rates g compared to cavity and qubit decay rates. Therefore, if the system is driven at its lowest resonance frequency $\omega_1 = \omega - g$ the only state that can be populated is $|1, -\rangle$. This means that the photon blockade system can be excited by a *single* excitation. Only once the system has relaxed back into the ground state by emitting a single photon it can be excited again. Therefore the frequency ω_1 will be chosen to be the working frequency of the system. This system was already experimentally realized by our group by using a superconducting qubit coupled to a microwave resonator [4].

2.2 Parametric Drives

The purpose of this component is to emit two single photons simultaneously into two adjacent cavities. This can be realized by a qubit-like system that has energy levels as sketched in Figure 2.1b coupled to two photon blockade systems. When the qubit-like system is in its second excited state $|f\rangle$ it cannot decay into its first excited state $|e\rangle$ since the transition frequency is not resonant with the photon blockade systems. It is forced to decay into its ground state $|g\rangle$ emitting two single photons of the frequency ω_1 , one into each adjacent cavity.



(a) Energy levels of a cavity coupled to a qubit. The non-linearity of this system allows the construction of photon blockades.

(b) Energy level diagram of the qubit-like system.

Figure 2.1: The two relevant energy level schemes for our samples. At our working frequency ω_1 the only allowed processes are the single-photon transition between $|0\rangle$ and $|1, -\rangle$ in the photon blockade system, and the two-photon transition between $|g\rangle$ and $|f\rangle$ in the parametric drive.

In the experiment, one possible issue is the excitation of the system into the $|f\rangle$ state, since the transition $|g\rangle \rightarrow |f\rangle$ is forbidden for single-photon processes in our eventual realization of the device. This means that it has to be excited through a two-photon process. However, if we want to excite it using only one frequency, we would have to use the frequency ω_1 which is exactly the working frequency of the photon blockade systems. Therefore the coupling of the driveline to the parametric drive must be much bigger than the coupling of the drive-line to the photon blockade systems. An alternative solution to this problem could be to use two different drive frequencies, e.g. one for the transition $|g\rangle \rightarrow |e\rangle$ and another one for the transition $|e\rangle \rightarrow |f\rangle$, or any other two frequencies that sum to $2\omega_1$.

3 Components

The parametrically driven nonlinear resonator chain has been realized in several samples. There is one set of 6.6 mm by 7 mm samples with two to six resonators and another set of 4.3 mm by 7 mm samples with only two resonators. All of these samples have very similar basic components, as will be explained in this section.

3.1 Resonator

The resonators that will be used in the samples are coplanar waveguides, i.e. two-dimensional coaxial cables, with their length chosen to correspond to a resonance frequency of 7 GHz, and their central conductor width and full width chosen to match an impedance of 50Ω to ensure compatibility with commercially available microwave engineering equipment.

3.2 Qubits

The qubits that will be used in the experiments are known as transmons [5]. I will not further describe their internal design since they are written using e-beam lithography and we only have to reserve some space for the transmons during the mask design.

The coupling of the qubit to the resonator is realized by capacitive coupling of the electric dipole moment of the qubit to the electric field of the resonator. Thus, the coupling strongly depends on the placement of the qubit relative to the resonator because it is proportional to the electric field. A stronger coupling can be achieved by placing the transmon closer to the central conductor and close to an antinode of the resonator. The geometry of the 6.6 mm by 7 mm samples does not allow the placement of the qubit directly at an antinode, therefore the qubit is placed at $1/4$ of the resonator length. The coupling of the qubit to the single-photon mode of the resonator is proportional to the electric field of the resonator, thus is smaller by a factor of $\cos(\pi/4) = 1/\sqrt{2}$. A stronger coupling can be measured more easily which is desirable for the experiment.

3.3 Flux Gatelines

The flux gatelines or fluxlines are coplanar waveguides that pass close to the superconducting loop of a qubit and then go to an electric ground, so that a small current sent through the line will create some magnetic flux through the area enclosed by the loop, which allows one to tune the resonance frequency of the qubit. Since the only purpose of these lines for the desired experiment is to create an adjustable local magnetic flux, it is possible to replace some fluxlines by the same number of external sources of magnetic fields. Currently, up to four small superconducting coils can be placed below the sample holder of the chip for this purpose.

3.4 Charge Gatelines

The charge gatelines or chargelines are lines that couple capacitively to the island of the qubit or qubit-like system, which enables one to excite the qubit or qubit-like system using microwave radiation. This type of line is necessary for the parametric drives, as this is how the system will be excited in the final experiment.

The photon blockade qubits need not to be excited by any gate line in the final experiment, they only have to couple to the resonator to provide a nonlinearity to the resonator. Therefore, the chargelines are not necessary for the photon blockade qubits. They are still useful for performing other tests on the sample though, such as for characterizing qubit and resonator properties and calibrating some parameters.

3.5 Airbridges

Airbridges are small pieces of superconducting wires that are placed above the coplanar waveguides on the sample. They connect the two parts of the ground planes of the coplanar waveguide, such that there is a ground plane at a well-defined electric potential. The samples are produced by removing the aluminum along the empty areas of the masks, so that there are isolating parts in the layer of superconducting aluminum. Therefore, if one simply drew out all the coplanar waveguides on the sample, the ground plane would be cut into several fragments, that might be at different electric potentials. However, it is necessary for the coplanar waveguide resonators to have a single ground plane at well-defined electric potential. Therefore, there are airbridge structures across all coplanar waveguides on the sample, i.e. small aluminum wires that are $2\ \mu\text{m}$ above the sample, such that a current could compensate for any voltage difference.

Placing the airbridges on the samples, one must take care not to create any small closed superconducting loops around the qubits. In earlier experiments, hysteretic effects have been observed when tuning the qubit transition frequency using magnetic flux if there are small closed superconducting loops around it. The magnetic fluxes that are used to tune the qubit transition frequency are smaller than the magnetic flux quantum $\Phi_0 = \frac{h}{2e}$. Therefore, this hysteresis is not due to the Meissner-Ochsenfeld effect, which can only compensate for integer multiples of the magnetic flux quantum.

An alternative to airbridges created using optical lithography are bond wires that are connected to the ground planes by hand using a bonding machine, which is microscope and special tweezers. Placing the wires by hand is far less exact than writing them using photolithography. However, for this experiment the resonators are required to be very close copies of each other. Therefore we decided to use airbridges instead of bond wires, which change the capacitive environment of the resonators more reproducibly.

4 Mask Design with Mathematica

The masks for the photolithography are created using 3D graphics files. These 3D graphics used to be designed manually using CAD software. However, in order to design complicated samples with many repeated structures, further automatization is possible and necessary. For this purpose the Qudev group has written a Mathematica library for mask design, which is under constant development.

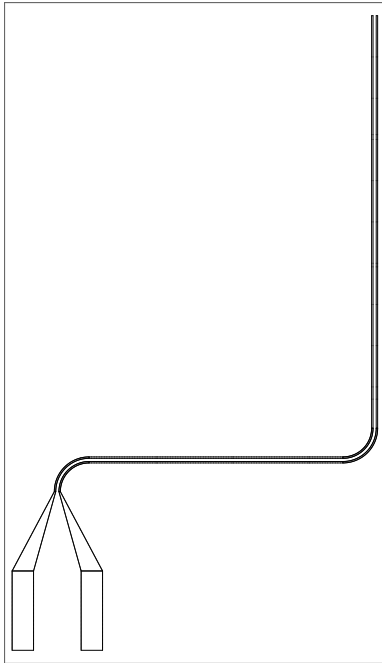
4.1 Semiautomatic Gateline Placement

When I started to work on this semester thesis, there were two ways to draw a coplanar waveguide. The first way was to create each straight or curved segment individually at the correct locations. The other way was to use a function that would create a 90° curve, go straight on for a defined length, then create another curve that goes back to the initial direction and further on for a defined length. Based on this function, I wrote a function that would draw a coplanar waveguide with not just one but an arbitrary number of arbitrarily long straight segments in x and y directions. Also, every function used only internal parameters of the coplanar waveguide they draw, i.e. widths, lengths, radii, etc. The object then had to be moved using a separate function. This meant that one has to compute all those parameters from the coordinates of the coplanar waveguide before being able to draw the coplanar waveguide. In order to speed up the process of connecting the basic components to the input and output ports of the chip, I wrote a function called `ConnectLines`. It would take the coordinates of the starting point, the ending point of the line, the angles at which to approach start and endpoint and connect them, based upon the function discussed previously. The `ConnectLines` function itself cannot take other structures into account, but one can give the function additional coordinates that the coplanar waveguide has to go through in order to avoid crossing of other parts of the sample, which makes use of the option of the first function to have any number of segments, as can be seen in Figure 4.1. Also, for both these functions, I have written two additional functions: one draws airbridges across the structure and one computes the length of the structure, which can be used to calculate the resonance frequency of the waveguide in order to avoid unwanted resonances on the chip.

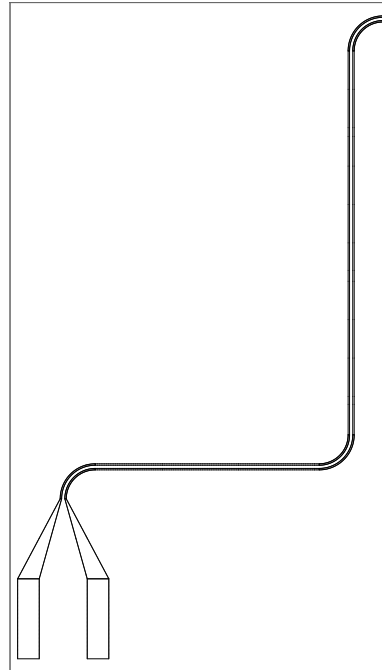
4.2 “Black Boxes”

The masks designed using Mathematica are only used for photolithography, not for e-beam lithography. Therefore there are rectangles surrounded with markers for elements that will be written using e-beam lithography after the photolithography processing (“black boxes”). This is necessary for elements that are too small for photolithography, since the resolution of any optical process is limited not only technologically but also by the wavelength of the light that is used to structures that are at least $2\ \mu\text{m}$ in size. Also, since the e-beam lithography can be done at any later time, having black boxes as placeholders for some elements adds variability to the samples, because after experimenting on one sample that was produced from the *same* wafer one might want to vary some parameters before testing the next sample.

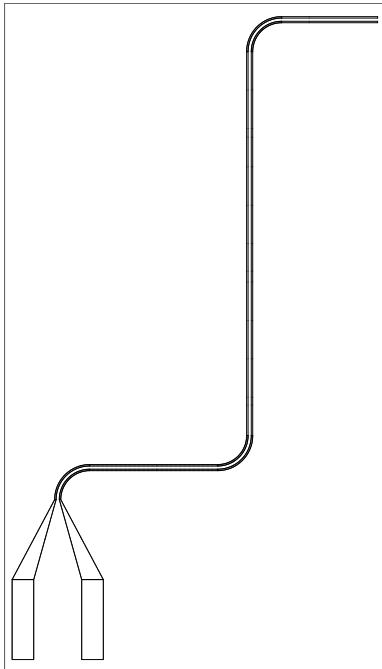
(a) `ConnectLines[{0, 0}, 0, 75, a1/b1, {1000, 2000}, 0, a1, a1/b1, 0, 0, {}]`



(b) `ConnectLines[{0, 0}, 0, 75, a1/b1, {1000, 2000}, $-\pi/2$, a1, a1/b1, 0, 0, {}]`



(c) `ConnectLines[{0, 0}, 0, 75, a1/b1, {1000, 2000}, $-\pi/2$, a1, a1/b1, 300, 0, {}]`



(d) `ConnectLines[{0, 0}, 0, 75, a1/b1, {1000, 2000}, $-\pi/2$, a1, a1/b1, 300, 0, {{400, 1000}, {700, 1500}}]`

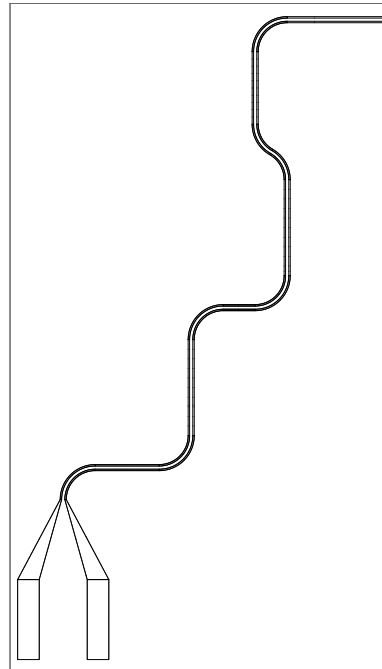


Figure 4.1: Four examples of usages of the `ConnectLines` function: (a) Connecting a port at $(0, 0)$ to $(1000, 2000)$. The graphic is created from the line of code above. (b) Compared to (a), the orientation of the upper end of the line has been rotated clockwise by $\pi/2$ (c) Compared to (b), a straight segment of $300 \mu\text{m}$ has been attached to the upper end of the line. (d) Compared to (c), two points ($(400, 1000)$ and $(700, 1500)$) have been added, which the line now goes through.

There are three elements that are created using e-beam lithography. The qubits have some very small substructures i.e. Josephson junctions. The parametric drives are not yet completely designed and need Josephson junctions as well. Since it is unknown what capacitances are best used for the coupling of the resonator chain to the output, these capacitors are replaced by black boxes on some samples. For the other samples a capacitance of 6.6 fF was used, which is approximately the capacitance that would make the width (full width at half maximum) of the resonance peak equal to 1 MHz if the resonator is not coupled to anything else. Also there are some simple samples using a capacitance resulting in a 10 MHz wide resonance. Our group has never used such big capacitors, therefore we simulated the electric field in the structure using the electromagnetic field simulation software Maxwell. We then calculated the capacitances of multiple capacitors with various numbers and sizes of fingers.

In order to create a superconducting contact between the niobium structure written using e-beam lithography and the aluminum structure written using optical lithography, the structures need to overlap for at least $50\ \mu\text{m}$. This is required for the parametric drives, because they couple to two adjacent resonators, and for the output capacitors, since they couple the resonator chain to the output port.

4.3 Mask Completion for Ordering

After designing every single sample, one has to decide how many copies of each sample to place on the full mask and arrange them in a way such that any two copies of the same sample are not too close to one another in case the wafer is defective at one position.

This gives the final output of the Mathematica procedure. It is four 3D graphics files, one for the elements that will be directly on the wafer, one for the feet of the airbridges, and two for the airbridges themselves. After exporting these four files, they require further processing, which was done using the 3D graphics editing programs AutoCAD and LinkCAD.

At first all lines had to be given finite width and all open polygons had to be closed, this was done by using the Repair function in LinkCAD. Then the two masks for the Airbridges had to be subtracted from one another, this was done by at first using AutoCAD to put both masks into different layers of one file, and then subtracting the layers from one another using LinkCAD. Then finally the repaired and subtracted masks are merged with a template containing test structures and alignment markers along with a mask identification string.

5 The Samples

If several resonators with photon-blockades are coupled using the parametric drives as explained above, it is expected to be able to observe Majorana bound states of microwave radiation [1].

Therefore, the goal of this project was to design chips that hold as many resonators with the necessary additional devices, i.e. qubits for the photon blockade and parametric drives, as possible given the dimensions of the sample and the number of ports on the sample holder. In order to be able to test the basic properties of the samples, some simpler and smaller samples are needed that have the same basic design but less resonators.

Therefore, the best approach was to first design the basic components that are used in almost all of the samples. Then, these building blocks are simply placed next to each other on a sample, and all the necessary connections are added.

The first task was to come up with a shape for the resonator that would allow placing as many copies of the resonator as possible on a single sample. The restrictions to the resonator were its length, because this defines its resonance frequency, and some free area is necessary for qubits, parametric drives, and gatelines to each of these elements. Ideally, one should be able to place six resonators on one 6.6 mm by 7 mm sample, which was first achieved using the design shown in Figure 5.2.

After designing the building blocks of the samples, a first version of the 6.6mm by 7mm sample with six resonators (see Figure 5.3) and a simplified version of this sample with only two resonators was designed, as a base for discussions with other group members and as a guideline for the samples with less resonators. The discussions led to some small modifications to the shape of the resonator (c.f. Figure 5.4), but no major changes in the design. The changes are explained in the caption of Figure 5.4.

The next step was to design samples with various smaller numbers of resonators but the same basic design, so that once the experiments on a smaller sample are successfully completed one should to be able to move on to the next sample with one more resonator. To avoid possible issues there should be as few changes as possible, thus the building blocks are left unchanged. This led to the design of samples with two to five resonators, c.f. Figures 5.8, 5.9, 5.10, and 5.11. Additionally, one sample with four resonators was designed that has only one parametric drive, which is placed between the two resonators in the middle, and only two qubits, attached to the two resonators in the middle, making the two outer resonators “buffer” resonators, c.f. Figure 5.12. In an earlier stage of the theoretical work by Bardyn et

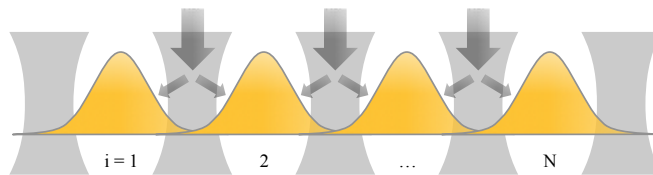


Figure 5.1: Parametrically driven chain of nonlinear resonators, taken from [1].

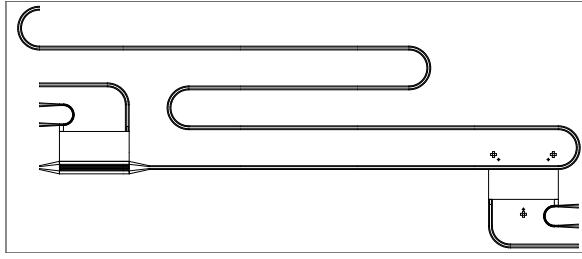


Figure 5.2: First resonator design with qubit (right) and parametric drive (left) that was compact enough to allow the placement of six resonators on a single chip. At this stage, the drive was visualized as a box and a resonator coupling capacitor, although it would be one big box in the final design.

al., the buffer resonators were discussed as a necessary condition to be able to observe the Majorana states.

In order to realize the experiment in a simpler geometry, a smaller 4.3 mm by 7 mm sample with two photon blockade systems was designed. This sample is supposed to be used with our groups standard sample holder to show that the experiment can work and to possibly avoid unwanted resonances that can appear in more complex arrangements.

Finally, a modified version of the smaller sample was designed with a beam splitter at the output of one resonator, which can be useful to show various properties of the output signal e.g. that the parametric drive emits exactly one photon into each resonator, using correlation function measurements as proposed in [6].

For each regular sample, i.e. no beam splitters or buffer resonators, there are three versions: version one has boxes for the parametric drives and 1 MHz couplers between resonator and output (c.f. Figure 5.5); on version two the output couplers are replaced by “black boxes” for reasons given in Section 4.2 (c.f. Figure 5.6); and on version three the boxes for the parametric drives are replaced by 10 MHz couplers (c.f. Figure 5.7). For the small regular sample, there is an fourth version on which the parametric drive is replaced by a 1 MHz coupler. For the samples with a beam splitter or with buffer resonators, there are only versions with only boxes, because the coupling between the various parts of the resonator chain is not known yet.

Versions one and two, which both have parametric drives, can be used in the final experiments, with the only difference that in the version with only boxes the output coupling capacitor can be designed by e-beam lithography.

Version three mainly serves the purpose of identifying unwanted resonances or other errors. Also, there will be no niobium qubits written into the black boxes, which enables one to test the device at higher temperature since niobium has a lower critical superconducting temperature than aluminum. This means the sample can be measured relatively quickly with a dipstick in liquid helium at 4 K.

For the final mask, we chose to omit the samples with five and six resonators in order to be able to have enough copies of each sample with four or less resonators. The samples with five and six resonators will most probably be added to another mask in the future. The final mask including the test structures ready to be ordered is shown in Figure 5.15.

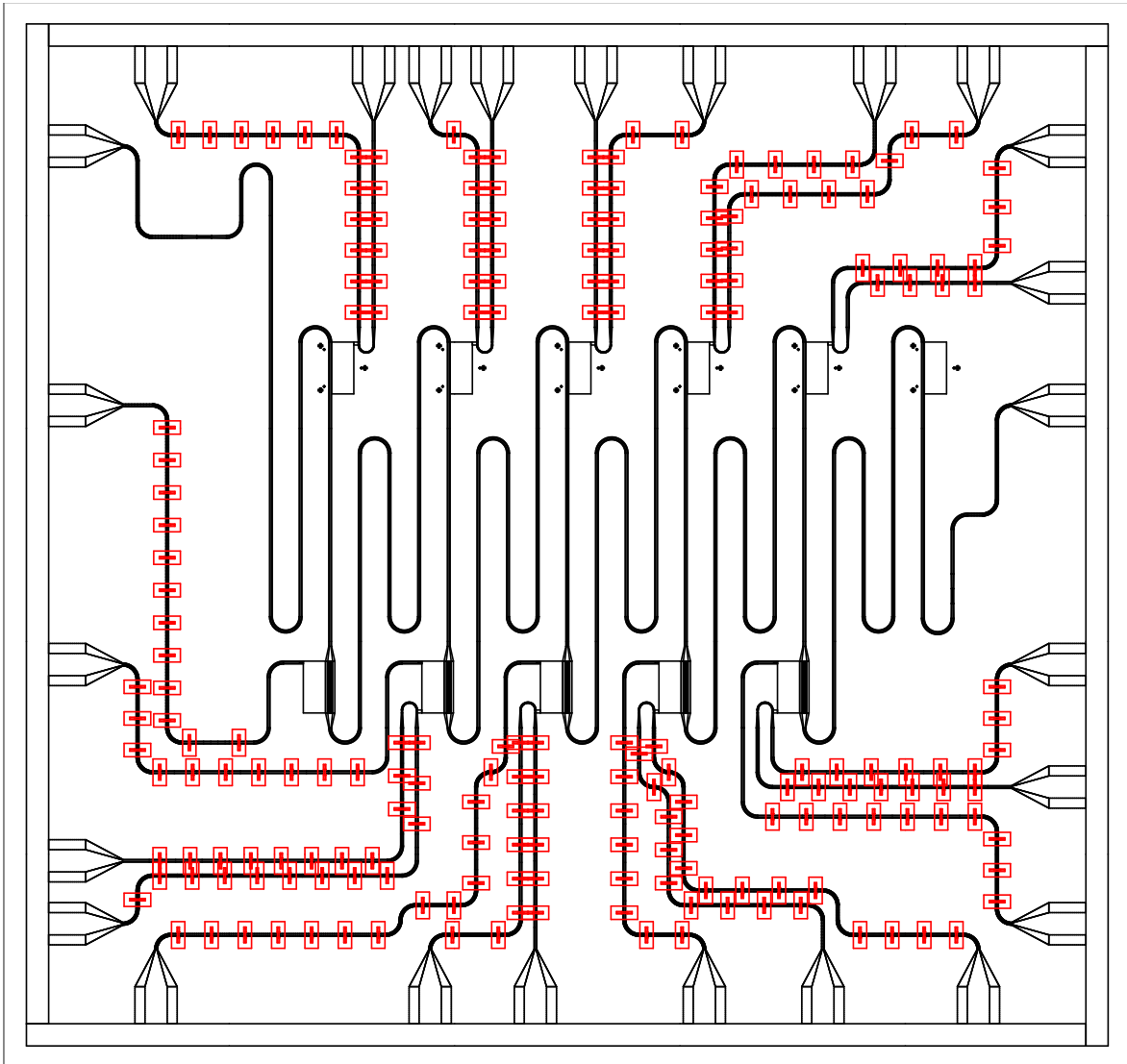


Figure 5.3: First design of a sample with six resonators, using the first resonator design. The boxes on the upper half of the sample are the qubits for the photon blockade, the boxes on the lower half are the parametric drives. The circuit is sketched in Figure 5.5.

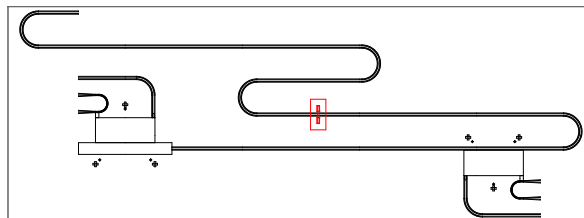


Figure 5.4: Final design of the resonator with qubit and parametric drive. The difference between the older resonator shown in Figure 5.2 and this one is that the placement of the qubit is now fixed at $1/4$ of the resonator length, and there is more space between the fluxlines and the resonator. The airbridge is placed in the center of the resonator to maximize the size of any superconducting loops around SQUIDS in the qubits and parametric drives.

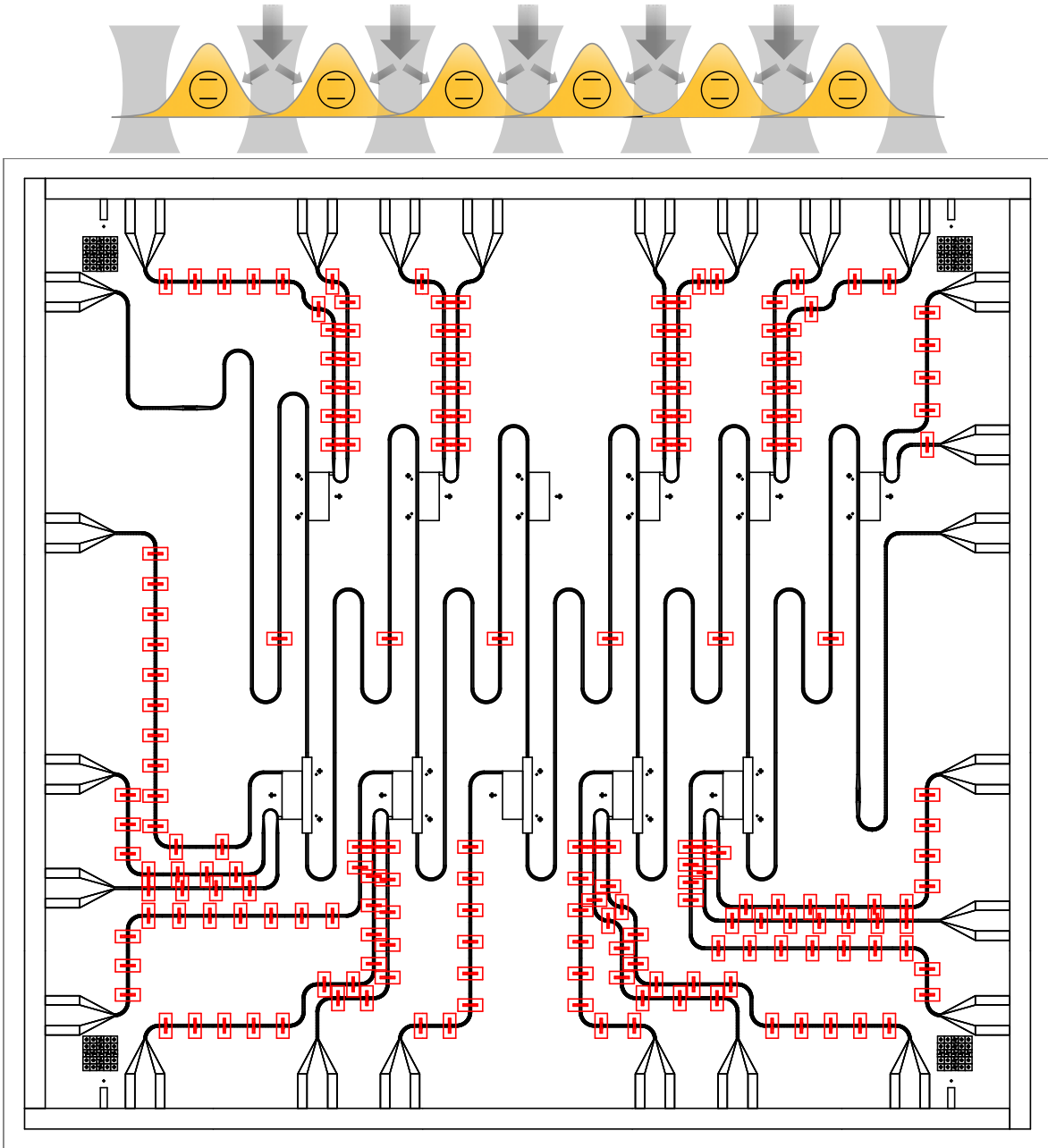


Figure 5.5: Top: Sketch of the system with six parametrically driven cavities each coupled to a two-level system. Adapted from [1]. Bottom: Final design for the sample with six resonators. The qubits for the photon blockade are on the upper half, the parametric drives are on the lower half. The charge lines to the qubits are missing because the qubits are only needed to provide the nonlinearity for the resonators and do not need to be excited via a gateline. The two missing fluxlines to the third qubit from the left and the third parametric drive from the left are compensated for using coils placed underneath the sample. If these gatelines had not been left out we would have needed more input ports on the chip than we have available. In this version of the sample there are capacitors for the output coupling and boxes for the parametric drives.

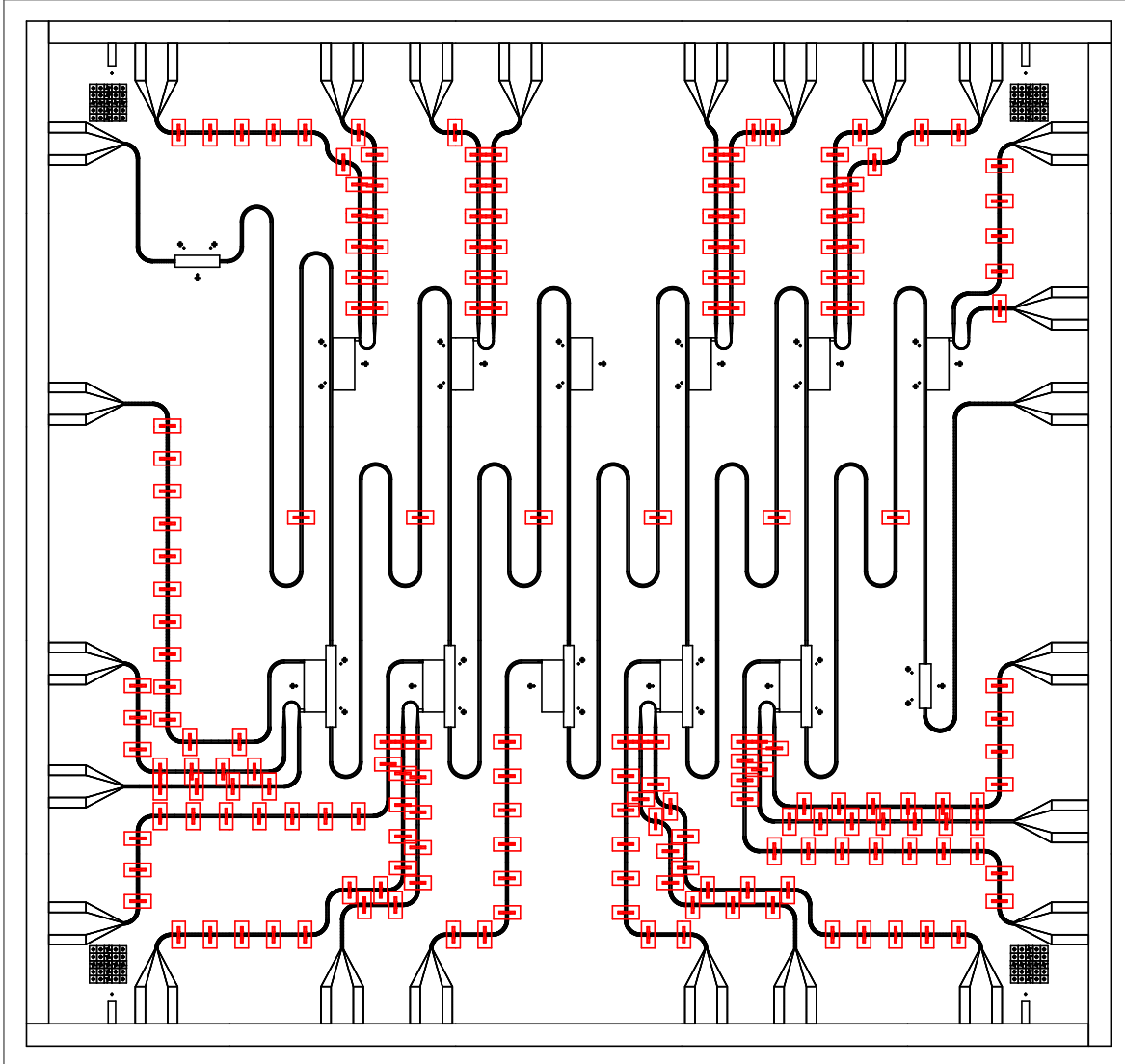


Figure 5.6: The same design as shown in Figure 5.5, but the capacitors at the outputs are replaced by black boxes. This allows us to use different capacitances depending on the results of future measurements.

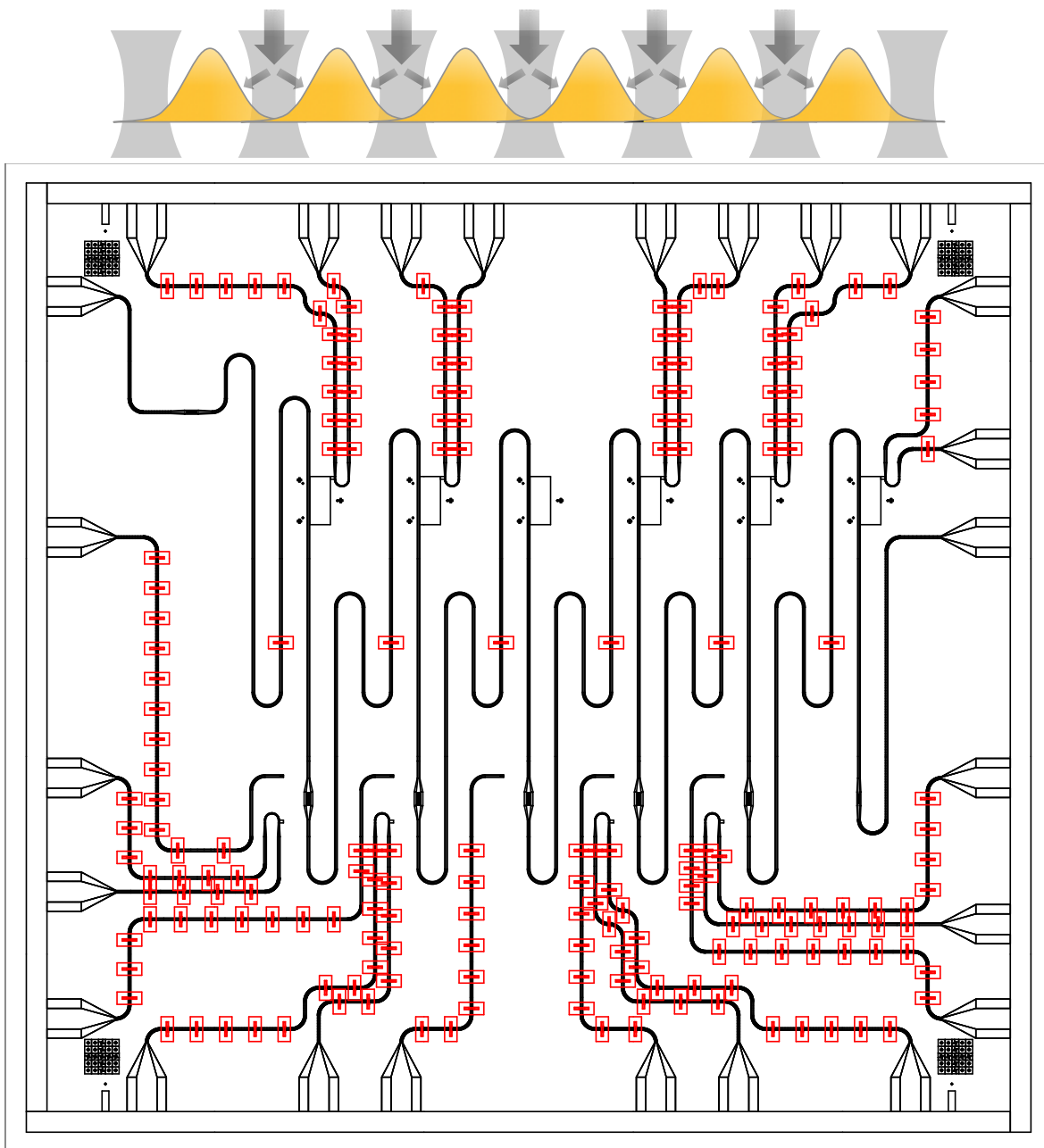


Figure 5.7: Top: Sketch of the system with six parametrically driven cavities without the two-level systems. Bottom: The same design as shown in Figure 5.5, however the parametric drives are replaced by capacitors. This version is intended for testing the design in a dipstick measurement in liquid helium.

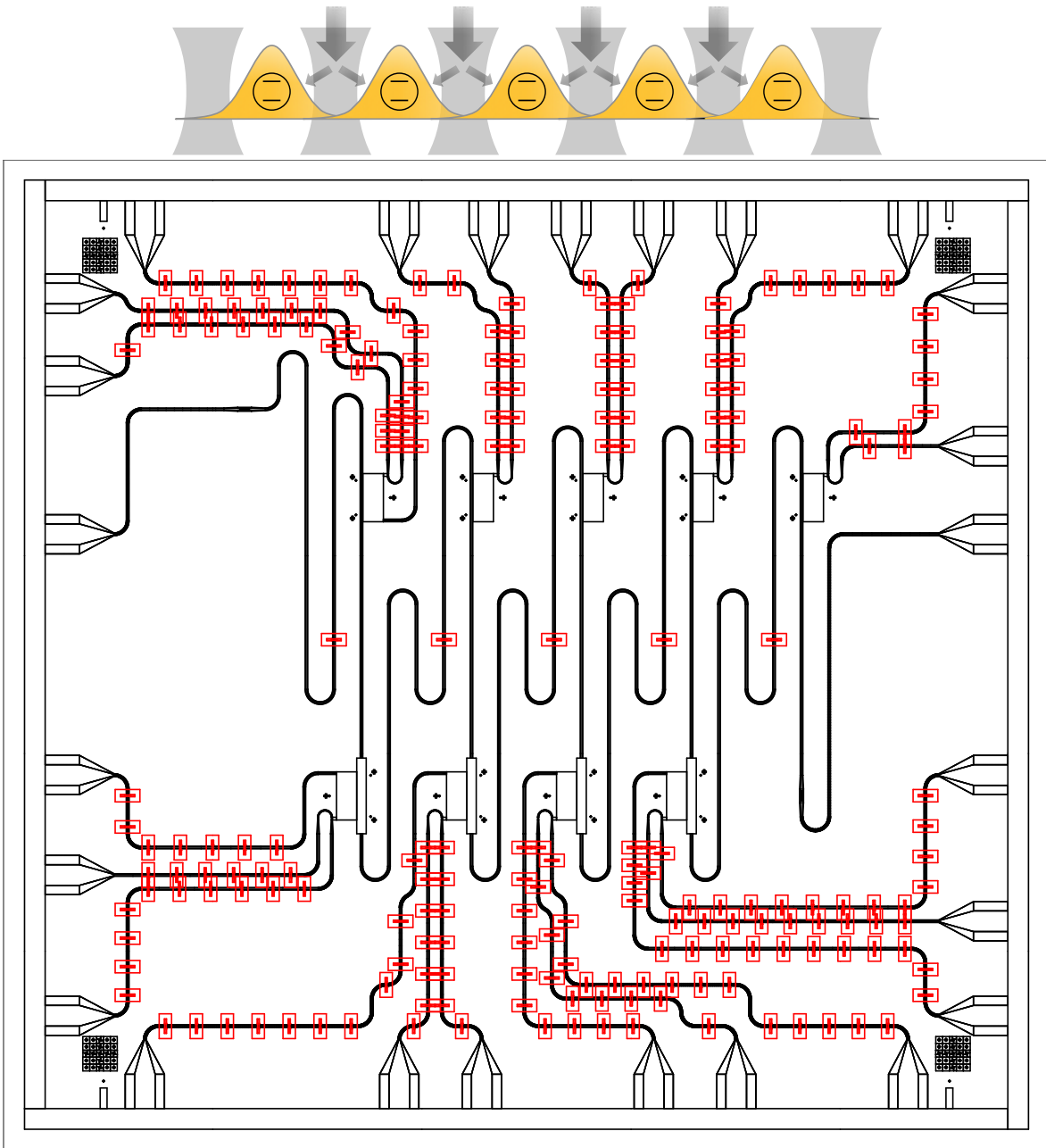


Figure 5.8: Top: Sketch of the system with five parametrically driven cavities each coupled to a two-level system. Adapted from [1]. Bottom: Final design for the sample with five resonators. The qubits for the photon blockade are on the upper half, the parametric drives are on the lower half. The chargelines to four of the qubits are left out because they are not necessary, since the qubits are needed only for the photon blockade and do not need to be driven by any additional gatelines. We had to leave out these four gatelines because there are only 16 ports available on the chip.

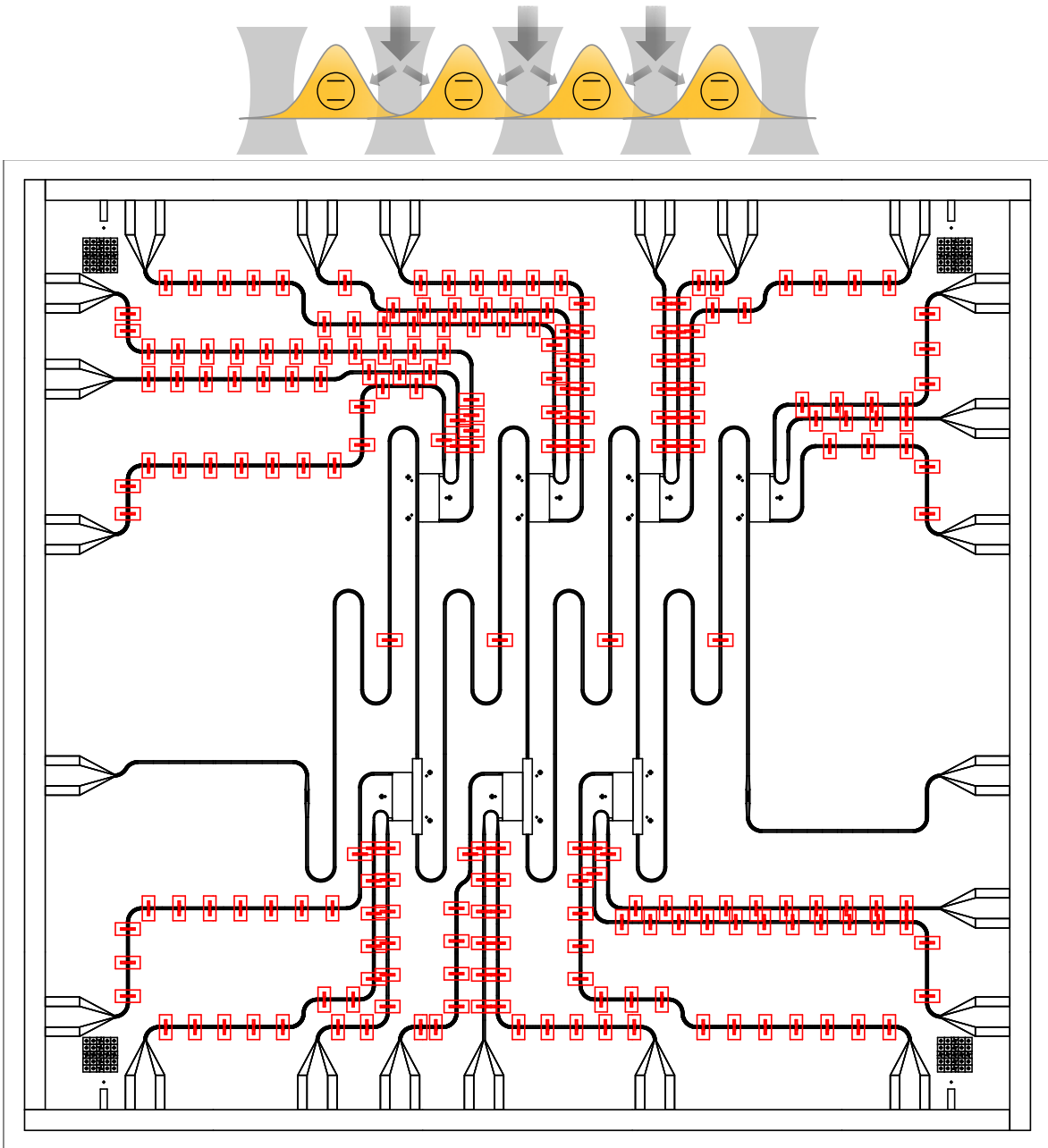


Figure 5.9: Top: Sketch of the system with four parametrically driven cavities each coupled to a two-level system. Adapted from [1]. Bottom: Final design for the sample with four resonators. The qubits for the photon blockade are on the upper half, the parametric drives are on the lower half.

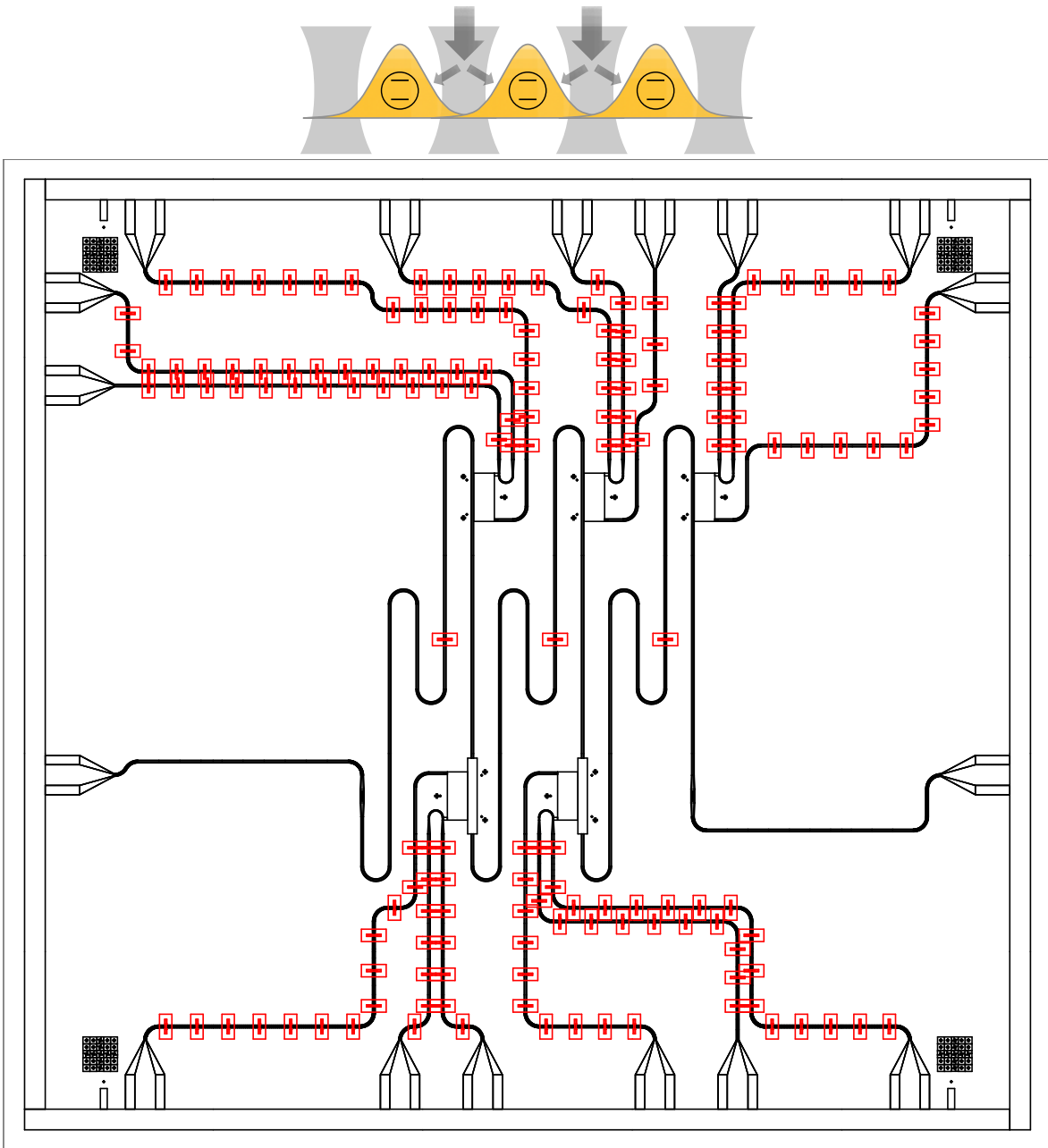


Figure 5.10: Top: Sketch of the system with three parametrically driven cavities each coupled to a two-level system. Adapted from [1]. Bottom: Final design for the sample with three resonators. The qubits for the photon blockade are on the upper half, the parametric drives are on the lower half.

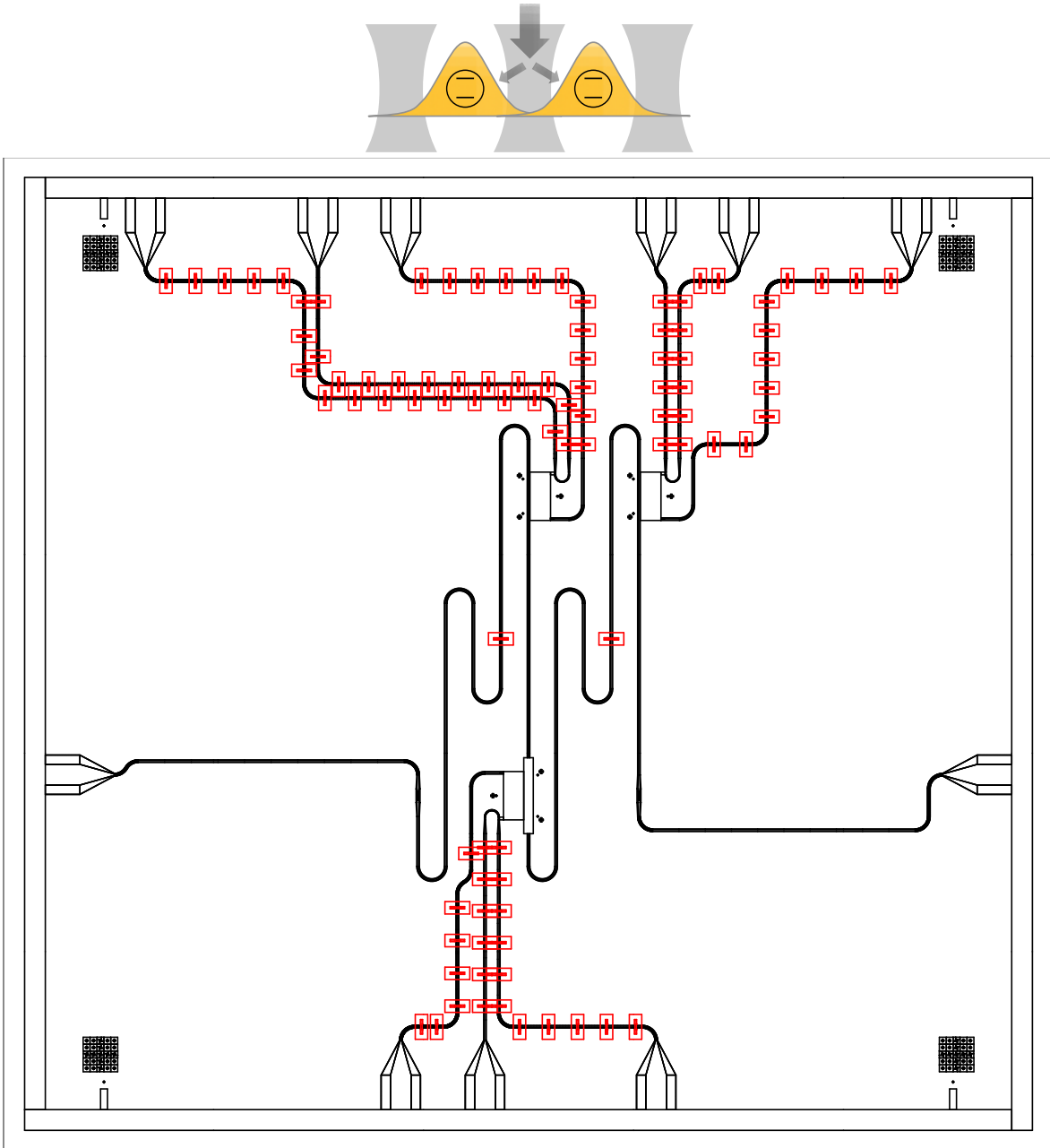


Figure 5.11: Top: Sketch of the system with two parametrically driven cavities each coupled to a two-level system. Adapted from [1]. Bottom: Final design for the sample with two resonators. The qubits for the photon blockade are on the upper half, the parametric drive is on the lower half.

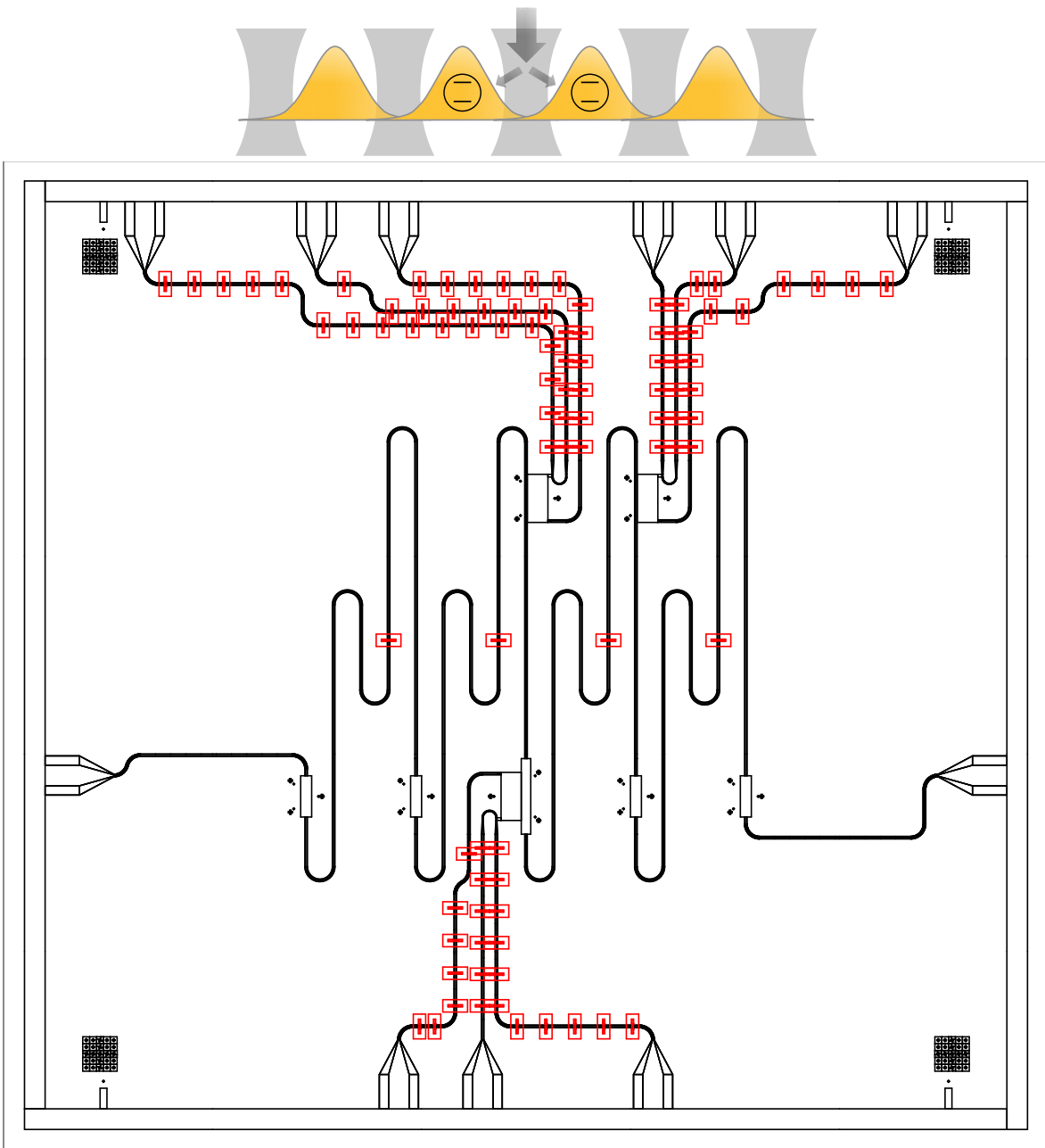


Figure 5.12: Top: Sketch of the system with two parametrically driven cavities coupled to a two-level system and two probe cavities at each end. Adapted from [1]. Bottom: Sample with two resonators with photon blockades and a parametric drive and two resonators serving as buffers. The qubits for the photon blockade are on the upper half, the parametric drive is on the lower half.

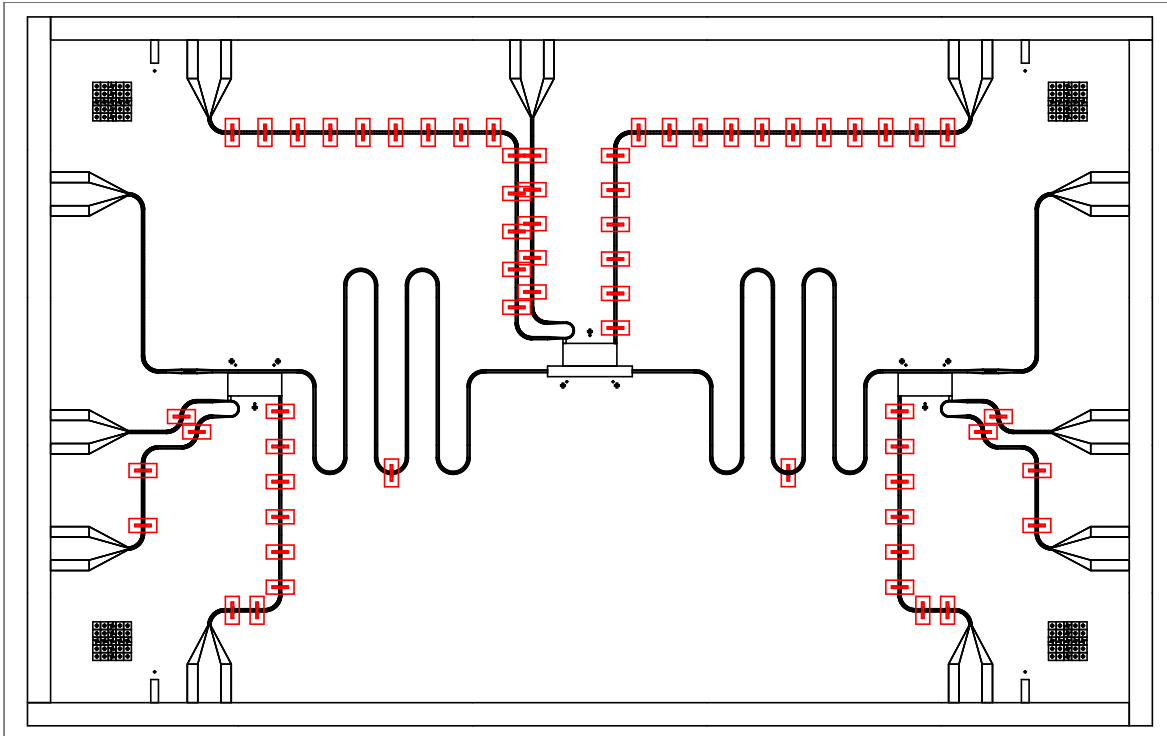


Figure 5.13: Smaller sample (4.3 mm by 7 mm) with two resonators (middle). The parametric drive is in the center. The qubits are close to the left and right ends of the sample. The circuit is equivalent to the one shown in the sketch and on the sample in Figure 5.11.

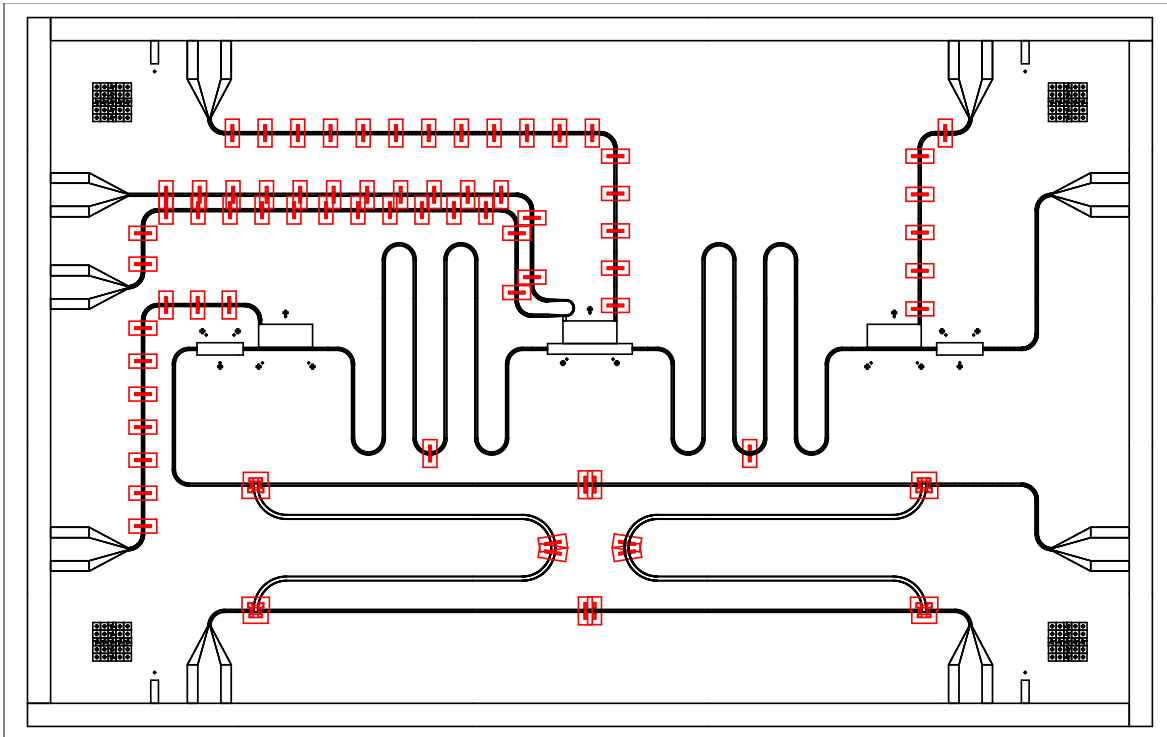


Figure 5.14: Smaller sample (4.3 mm by 7 mm) with two resonators (middle) and a beam splitter (bottom) at one output. The parametric drive is in the center. The qubits are close to the left and right ends of the sample.

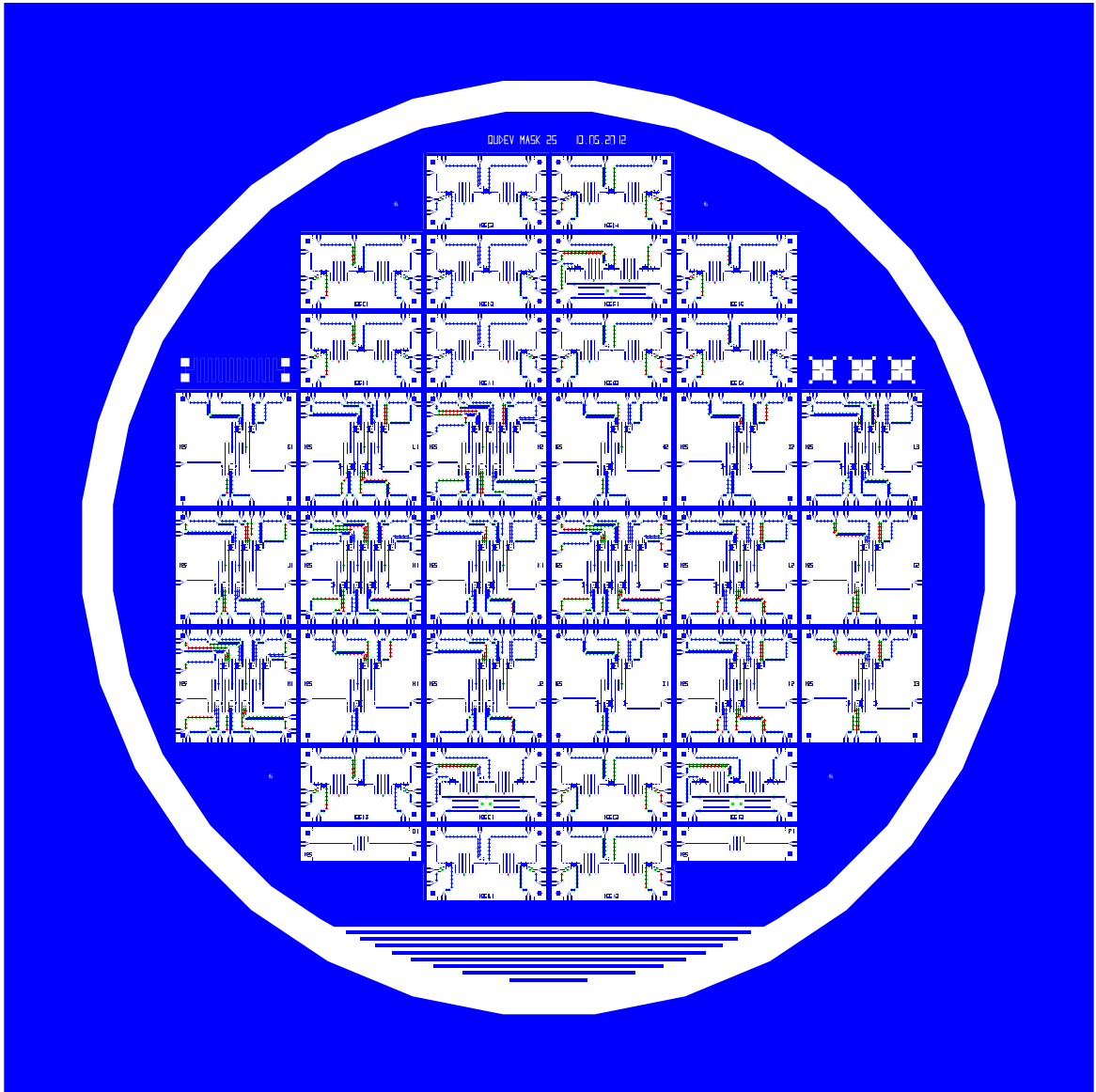


Figure 5.15: The final mask that has been ordered. The lowest layer, which contains the waveguides and black boxes, is blue. The middle layer, which contains the feet of the airbridges, is green. The top layer, which contain the airbridges, is red.

6 Conclusion and Prospect

The goal of this semester thesis was to design a series of microwave circuits that could serve for the experimental study of Majorana bound states of light in circuit QED. In order to achieve this goal, a new compact form for microwave resonators that allows the placement of six resonators along with six qubits and five parametric drives on one 6.6 mm by 7 mm sample was developed. 21 different circuits were designed, five of which for a 4.3 mm by 7 mm sample and 16 for a 6.6 mm by 7 mm sample. All samples were designed using Mathematica with a library that was created by the Quantum Device Lab group. Whilst designing the samples, some additions to this library had been made.

The purpose of using a photon blockade system, consisting of a harmonic resonator and a qubit, is to create a system that can be excited to its first excited state but no higher energy levels as long as it is excited with a suitable frequency. Such a system could be replaced by an inherently anharmonic resonator. This would mean that the resulting basic repeated component would be smaller because there is no additional qubit, which in turn would allow one to create longer chains of resonators. The frequency of the resonator as to be tuned nevertheless by magnetic flux through the SQUIDs. Such an anharmonic resonator could be realized by creating a coplanar waveguide resonator with a small structure in the central conductor that shows non-linear behaviour, such as a SQUID.

This semester thesis was my first work in a research group, and it was a very valuable experience to me since it allowed me to see a research group from the inside for the first time. It has shown me a very practical approach to physical problems as opposed to the mostly theoretical approach of the courses of the bachelor curriculum. I have seen how to implement a very abstract quantum mechanical system in a real superconducting microwave circuit.

During the work on the semester thesis, I have greatly improved my skills with Mathematica and have seen some basic CAD.

I would like to thank Prof. Andreas Wallraff for allowing me to do this semester thesis at the Quantum Device Lab, my supervisor Christian Lang for all the explanation and help with the problems I have encountered, Christopher Eichler for the helpful and detailed discussions and all the other members of the Quantum Device Lab for their advice and for providing a great working environment for me in the group.

Bibliography

- [1] C.-E. Bardyn and Ataç Imamoglu. Majorana bound states of light in a one-dimensional array of nonlinear cavities. *arXiv:1204.1238*, 2012.
- [2] A. Wallraff, D. I. Schuster, A. Blais, L. Frunzio, J. Majer, S. M. Girvin, and R. J. Schoelkopf. Approaching unit visibility for control of a superconducting qubit with dispersive readout. *Physical Review Letters*, 95:060501, 2005.
- [3] A. Blais, R.-S. Huang, A. Wallraff, S. M. Girvin, and R. J. Schoelkopf. Cavity quantum electrodynamics for superconducting electrical circuits: An architecture for quantum computation. *Physical Review A*, 69(6):062320, 2004.
- [4] C. Lang, D. Bozyigit, C. Eichler, L. Steffen, J. M. Fink, A. A. Abdumalikov Jr., M. Baur, S. Filipp, M. P. da Silva, A. Blais, and A. Wallraff. Observation of resonant photon blockade at microwave frequencies using correlation function measurements. *Physical Review Letters*, 106(24):243601, 2011.
- [5] Jens Koch, Terri M. Yu, Jay Gambetta, A. A. Houck, D. I. Schuster, J. Majer, Alexandre Blais, M. H. Devoret, S. M. Girvin, and R. J. Schoelkopf. Charge-insensitive qubit design derived from the Cooper pair box. *Phys. Rev. A*, 76(4):042319, 2007.
- [6] Marcus P. da Silva, Deniz Bozyigit, Andreas Wallraff, and Alexandre Blais. Schemes for the observation of photon correlation functions in circuit qed with linear detectors. *Physical Review A*, 82(4):043804, 2010.